Structure of a Metal Ion Binding Site in β-Lactamase: Quantum Mechanical Study of the Influence of Hydrogen-Bonding Network and Backbone Constraints

Lars Olsen, Jens Antony, and Lars Hemmingsen*

Department of Mathematics and Physics, KVL, 1871 Frederiksberg C, Denmark

Kurt V. Mikkelsen

Department of Chemistry, University of Copenhagen, 2100 Copenhagen Ø, Denmark

Received: July 23, 2001; In Final Form: October 24, 2001

The structure and electric field gradients at the site with a histidine, an aspartic acid, a cysteine, and 1−2 water molecules as ligands are investigated with density functional and Hartree−Fock methods. This site has been shown experimentally to be occupied in the mononuclear cadmium-β-lactamase. Three types of model systems are studied: (1) the metal ion and the coordinating ligands, (2) the metal ion, the coordinating ligands and the local hydrogen-bonding network, and (3) the metal ion, the coordinating ligands, the hydrogen-bonding network, and the constraints from the surrounding protein. Good agreement with experimental data is obtained when optimizing systems 2 and 3, indicating that inclusion of the hydrogen-bonding network is important. The results suggest that the site is five-coordinated and structurally flexible.

1. Introduction

Bacteria have developed diverse defense mechanisms against penicillins and related antibiotics. In particular, this has become a problem during the past decades, in which certain pathogenic bacteria have become resistant to antibiotics. The primary defense mechanism is production of β-lactamases, which are enzymes cleaving β-lactam antibiotics. According to their amino acid sequences, β-lactamases have been grouped into four classes. While the enzymes from classes A, C, and D use an active site serine as the nucleophile, class B (or metallo) β-lactamases require a metal ion for catalytic activity. Metallo-β-lactamases have a broad substrate profile. In contrast to active site serine β-lactamases, no clinically useful inhibitors are yet available for metallo-β-lactamases.

The active site of metallo-β-lactamases contains two potential zinc binding sites.[1−9] For subclass B1, these are a site with three histidine residues (site 1) and a site with an aspartic acid, a histidine, and a cysteine (site 2).[10]

Concha et al. solved a structure of the β-lactamase from *Bacteroides fragilis* at 1.85 Å resolution containing two zinc ions in the active site (PDB code 1ZNB).[1] A solvent molecule bound to both zinc ions and is therefore most likely an OH^- at neutral pH in the binuclear enzyme. Furthermore, a second water molecule coordinates to the zinc in site 2 in an approximately trigonal bipyramidal geometry with the aspartate and the second water in apical positions. In the structure published by Carfi et al. (PDB codes 1BMI and 2BMI, resolution 2.0 Å), two zinc ions are found, but the shared water molecule is missing,[2] possibly because of the crystallization conditions with pH = 9. A crystal structure at 2.15 Å resolution for *B. fragilis* metallo-β-lactamase with two cadmium ions in the active site (PDB code 2ZNB) instead of two zinc ions has similar coordination geometry to the zinc enzyme,[3] and the metal−ligand bond lengths are longer. Inhibition of metallo-β-lactamase from *B. fragilis* by 4-morpholineethanesulfonic acid[4] (PDB code 1A7T) and a biphenyl tetrazole inhibitor[5] (PDB code 1A8T) does not change the ligands of the two zinc ions.

For metallo-β-lactamase from *Bacillus cereus*, a structure with only one zinc ion, which was bound to site 1, was solved in 1995 at 2.5 Å resolution with a water molecule coordinated to the metal ion (PDB code 1BMC).[6] In 1998, Carfi et al. solved a structure with two zinc ions (PDB codes 1BME and 1BVT) at 1.85 Å resolution.[7] Site 1 was fully occupied, while site 2 was only partially occupied. A carbonate ion is found instead of the second water in site 2. Furthermore, the first water molecule is only coordinated to the zinc ion in site 1. In the structure determined by Fabiane et al. (PDB code 1BC2, resolution 1.9 Å), the same ligands as in 1ZNB are found.[8] In ref 9, the structure of metallo-β-lactamase from *B. cereus* in which both zinc ions are four-coordinate is reported, that is, the second water molecule in site 2 is missing here. Consequently, the type and presence of the second solvent molecule at site 2 is not well-established.

It is currently not fully understood what the function of these two sites is, except that the metal ions are involved in the chemical reaction catalyzed by the enzymes.[11] In metallo-β-lactamase from *B. cereus*, the affinity for binding the second zinc is considerably lower than that for the first zinc ion.[12] In metallo-β-lactamase from *B. fragilis*, both zinc ions are about equally tightly bound.[13,14] Because the binuclear Zn^{2+} center of β-lactamase from *B. cereus*[8] is very similar to that of the enzyme from *B. fragilis*,[1] the difference between the binding affinities of the second zinc ion is most likely caused by differences in the near surroundings.[11] It is possible to exchange zinc with spectroscopic probes such as Co^{2+} [12−14] and Cd^{2+} [15,16] and still have catalytically active enzymes.

Recent studies of the activity showed that the metallo-β-lactamases from *B. cereus* and *B. fragilis* are active with only one zinc ion present in the active site, and full activity is reached with two zinc ions bound.[9,15,17] It has previously been assumed

* To whom correspondence should be addressed.

10.1021/jp0127972 CCC: $22.00
Published on Web 01/15/2002

that occupation of site 1 is the necessary requirement for catalytic activity both for the mono- and the binuclear enzyme (see for example ref 18). However, in a recent kinetic and spectroscopic study, it was shown that the mechanism for the mononuclear enzyme is different from the mechanism of the binuclear enzyme, illustrating the complexity of the system.[17]

In addition, recent kinetic, perturbed angular correlation of γ-rays (PAC) and NMR experiments indicate that for the mononuclear cadmium-substituted enzyme from *B. cereus* (1) some enzyme molecules have site 1 occupied and others have site 2 occupied and the enzyme is catalytically active under these conditions[9,17] and (2) the metal ion is jumping between the two sites on a time scale of 0.1−10 μs.[19] These findings further illustrate the complexity of the system and indicate that the conventional concept, that site 1 is responsible for catalytic activity, may be too simple a description. This raises the surprising possibility that occupation of site 2 is an integral part of the mechanism for the mononuclear enzyme. A thorough study of the coordination geometry of site 2 is a prerequisite for establishing models for a mechanism including this site. This is particularly important because X-ray diffraction and previous theoretical work show great variability in the coordination geometry of this site. In our work, we shall use the PAC spectroscopic signal from site 2 as an experimental reference to be reproduced by the theoretical studies.

A recent review of quantum mechanical studies of transition metal ions in biochemical systems can be found in Siegbahn and Blomberg.[20] In Diaz et al.,[21] quantum chemical calculations on model systems for the zinc ion binding sites in metallo-β-lactamase are performed at the HF, B3LYP, and MP2 levels of theory in vacuum with the 6-31G(d) basis set. In ref 22, the binuclear zinc- and cobalt-substituted metallo-β-lactamases are studied. The results indicate that the coordination number of the two cobalt ions remains the same as that of the zinc ions in the crystal structure. In ref 23, the mononuclear enzyme from *B. cereus* was investigated with the metal ion in site 1 using MD simulations. In ref 24, the binuclear active site of metallo-β-lactamase as a function of first and second shell water molecules is studied at the HF level or using polarizable molecular mechanics.

Here, we investigate the structure and PAC-spectroscopic properties of metallo-β-lactamase with only one metal ion in the binding sites (site 2) and how it is influenced by the local hydrogen-bonding network and constraints from the protein. It has previously been demonstrated that calculations of structure and electric field gradients (EFGs) are useful for the interpretation of PAC data from proteins.[25−30] We use the structure of β-lactamase from *B. fragilis*[1] as a starting point, but the results also have implications for the mononuclear enzyme from *B. cereus* and IMP-1[31] because their coordinating ligands are the same.

2. Method

All the calculations were performed with Gaussian 98, revison A.5 or A.7,[32] on PCs with Linux or SGI machines.

2.1. Structures. We have worked with three types of model systems for site 2: (1) the metal ion and the coordinating ligands, (2) the metal ion, the coordinating ligands, and the local hydrogen-bonding network, and (3) the metal ion, the coordinating ligands, the hydrogen-bonding network, and the constraints from the surrounding protein. In the following, they will be denoted "the small model systems", "the small model systems including the hydrogen-bonding network", and "the large model systems", respectively. The crystal structure of β-lactamase from

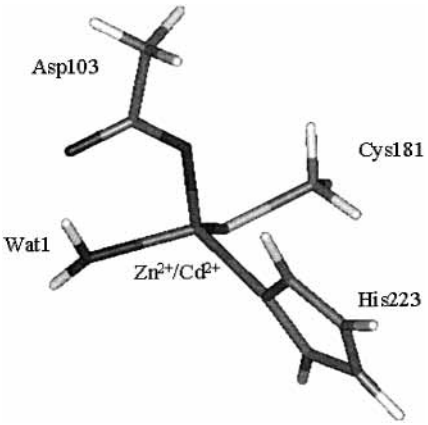

Figure 1. The small four-coordinated model system, $[ML_1]$. M^{2+} is used for either Zn^{2+} or Cd^{2+} and L_1^{2-} is used for $(CH_3COO)(CH_3S)(im)(H_2O)^{2-}$.

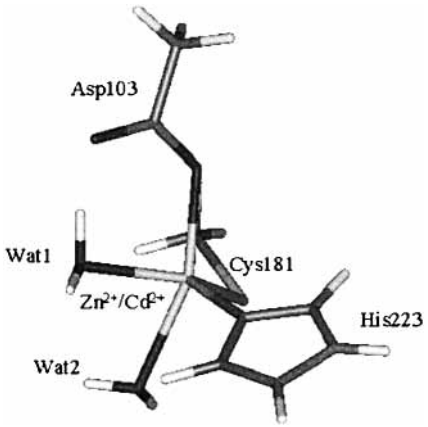

Figure 2. The small five-coordinated model system, $[ML_2]$. M^{2+} is used for either Zn^{2+} or $Cd^{2+}$and L_2^{2-} is used for $(CH_3COO)(CH_3S)(im)(H_2O)_2^{2-}$.

B. *fragilis*[1] (1ZNB) was used as a starting point for all structural analysis in this work.

The Small Model Systems. Site 2 was modeled as $[M(CH_3COO)(CH_3S)(im)(H_2O)]$ or $[M(CH_3COO)(CH_3S)(im)(H_2O)_2]$ with $M^{2+} = Zn^{2+}$ or Cd^{2+} and im = imidazole. In the following, we shall use $L_1^{2-} = (CH_3COO)(CH_3S)(im)(H_2O)^{2-}$ and $L_2^{2-} = (CH_3COO)(CH_3S)(im)(H_2O)_2^{2-}$. This gives the following short notation for the four- or five-coordinated small model system (i.e., with either one or two water molecules coordinating): $[ML_1]$ or $[ML_2]$, see also Figures 1 and 2.

The Small Model Systems Including the Hydrogen-Bonding Network. These model systems include the surrounding hydrogen-bonding water molecules in molecule A of the 1ZNB. We included two, three, four, and five additional water molecules, which are hydrogen bonding to the ligands: $[ML_2]\cdot(H_2O)_n$ with $n = 2-5$. For $n = 2$, Wat11 and Wat180 were included (see Figure 3, nomenclature as in the 1ZNB structure); for $n = 3$, Wat11, Wat180, and Wat5 were included; for $n = 4$, Wat11, Wat180, Wat5, and Wat101 were included; for $n = 5$, Wat11, Wat180, Wat5, Wat101, and Wat9 (Wat9 forms a hydrogen bond to the sulfur in Cys181) were included. However, with five additional solvent molecules, the geometry optimizations did not converge. Consequently, Wat9 was excluded from the model system.

The Large Model System. For the large model system, the atomic coordinates were taken from molecule A of 1ZNB. The molecular system was extended with the rest of the metal-coordinating amino acids and, in addition, one more amino acid

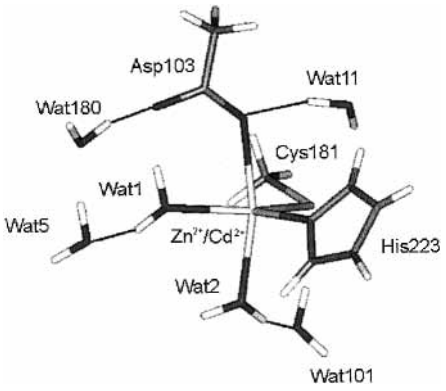

Figure 3. The model system including the hydrogen-bonding network, $[ML_2]\cdot(H_2O)_4$. Here, four additional water molecules from the crystal structure (1ZNB[1]) are included: Wat5, Wat11, Wat101, and Wat180. The black lines show the hydrogen bonds between the additional water molecules and the metal ion ligands.

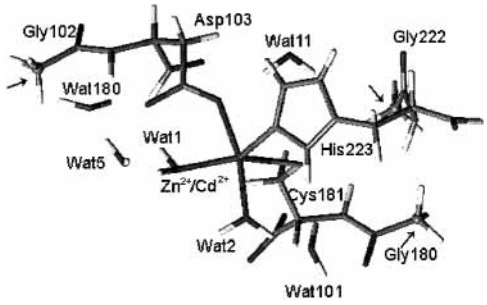

Figure 4. The large model system. The arrows show the three α-carbons that were fixed relative to each other in the geometry optimization.

for each metal ion ligand. The additional amino acids included in the large model systems were Gly102, Gly180, and Gly222 (the nitrogens next to the α-carbons in Gly102, Gly180, and Gly222 were not included in the calculation), see Figure 4. The α-carbons of the amino acids next to the metal ion-coordinating amino acid were frozen relative to each other.

We examined the distances from the α-carbons of Gly102, Gly180, and Gly222 to the metal ion in the 1ZNB and 2ZNB structures, where the latter contains cadmium instead of zinc. We found that these distances are 0.04, 0.14, and 0.29 Å longer in 2ZNB, respectively. On the basis of this and the fact that the cadmium ion has an ionic radius of about 0.2 Å larger than zinc, we chose the following strategy for constructing the large cadmium containing model system: The metal ion−ligand bond lengths were converted into typical cadmium ion bond lengths by moving the Gly102/Asp103, Gly180/Cys181, and Gly222/His223 fragments as rigid units. Typical cadmium ion−ligand bond lengths were chosen in accordance with ref 28.

The geometry optimization for the large model system was successful for the cadmium-containing system, but it did not work for the zinc-containing system (starting from the crystal structure). To geometry optimize a structure with zinc in site 2, the amino acids of the optimized large cadmium-containing structure were moved as a rigid unit such that the metal ion−ligand bond lengths again were according to 1ZNB. This structure was used as the starting point for an optimization. The consequence of this was that positions of the C_α atoms of the glycine amino acid residues were not exactly the same as in 1ZNB. This caused differences up to 0.8 Å in the distances between the frozen C_α atoms compared to those from the 1ZNB crystal structure.

2.2. Computational Details of the Electric Field Gradient Calculations. The EFG was calculated for the optimized cadmium-containing complexes. A nuclear quadrupole moment for ^{111m}Cd of 0.83 barn[33] was used to convert the measured nuclear quadrupole interactions (NQIs) to EFGs. When comparing with experiment, the eigenvalues of the EFG tensor are reported with $|V_{xx}| \leq |V_{yy}| \leq |V_{zz}|$, which is the usual convention. Only the absolute values are presented because the sign is not measured in $\gamma-\gamma$ PAC spectroscopy. Unless stated otherwise, the calculations of the EFG were performed on structures including only the metal ion-coordinating ligands, that is, $[CdL_1]$ or $[CdL_2]$, even though the optimizations may have been performed on a larger system.

2.3. Methods and Basis Sets. In most of the geometry optimizations, the B3LYP/LanL2DZ method was used.[34−38] No structural constraints were imposed in the geometry optimizations, except for the large model systems. Some optimizations, described below, were performed with larger basis sets and some at the Hartree−Fock level. The convergence criteria were the default values in Gaussian 98, except for the geometry optimizations at the Hartree−Fock level, which were stopped when the energies were converged within 10^{-5} au and the rms forces were smaller than 10^{-5} au.

Geometry optimizations with larger basis sets were performed for some of the cadmium-containing model systems: $[CdL_1]$, $[CdL_2]$, and $[CdL_2]\cdot(H_2O)_3$. The LanL2DZ basis set was still used on the cadmium, but either 6-31G(d) or 6-31+G(d)[39−43] was used on the ligands. In addition, a test calculation was performed in which a p and f function were added to the LanL2DZ basis set on Cd^{2+} with the exponents of 0.117 263 5 and 0.232 832 180 au, respectively.[25]

Geometry optimizations of the large model systems were performed with the two-layer ONIOM method of Morokuma and co-workers.[44−48] The high-level systems were $[ML_2]\cdot(H_2O)_4$. The low-level systems were the large model system described above. The B3LYP/LanL2DZ method was used for the high-level system, and PM3 was used for the low-level system.[49,50]

Unless otherwise stated, the EFG calculations were performed at the B3LYP level with the uncontracted basis set of Sadlej and Kellö[51] on cadmium and 6-31G(d) on the rest of the atoms (denoted S & K + 6-31G(d)) as in refs 25−28 and 30. The convergence criterion on the rms of the density matrix elements was 10^{-5} au as in ref 30.

3. Results

3.1. Structure of the Metal Ion Binding Sites. In Table 1, the geometry optimized structures of site 2 are presented. The first three rows show the results of the geometry optimized small model systems. For the $[ZnL_2]$ complex, it was not possible to geometry optimize a five-coordinated complex. The zinc ion-coordinating solvent molecule, Wat2, moved to make a hydrogen bond to CH_3COO^- or CH_3S^- after some cycles of the optimization. By removing Wat2, we constructed the four-coordinated $[ZnL_1]$ complex, which was then geometry optimized. In contrast to the corresponding zinc ion complex, the optimized $[CdL_2]$ complex remains five-coordinated. The geometry is approximately trigonal bipyramidal with Asp103 and Wat2 in the apical positions ($Asp103-Cd^{2+}-Wat2 = 163°$) and Wat1, Cys181, and His223 in a plane. The most notable difference from a perfect trigonal bipyramidal structure is observed for the $Asp103-Cd^{2+}-Cys181$ angle (122°). We also optimized a model system without Wat2, that is, a $[CdL_1]$ complex. Compared to the five-coordinated $[CdL_2]$ complex,

TABLE 1: Geometry Optimized Zn^{2+} and Cd^{2+} Containing Model Systems[a]

	distance to the metal ion (Å)					angle subtended at the metal ion (deg)						
	O1	O2	O103	S181	N223	O103−O1	O103−O2	O103−S181	O103−N223	O1−S181	S181−N223	N223−O1
Small Model System												
$[ZnL_1]$	2.04		2.04	2.36	2.11	90		134	95	113	111	111
$[CdL_1]$	2.26		2.24	2.50	2.33	85		133	95	127	114	91
$[CdL_2]$	2.24	2.52	2.30	2.60	2.30	83	163	122	84	120	114	123
Small Model System Including Hydrogen-Bonding Network												
$[ZnL_2]\cdot(H_2O)_2$	2.10	2.28	2.13	2.44	2.08	87	163	100	101	131	112	114
$[ZnL_2]\cdot(H_2O)_3$	2.03	2.28	2.17	2.46	2.08	87	168	99	98	133	111	113
$[ZnL_2]\cdot(H_2O)_4$	2.03	2.17	2.24	2.48	2.10	83	166	94	92	128	108	123
$[CdL_2]\cdot(H_2O)_2$	2.44	2.40	2.33	2.57	2.28	81	144	100	104	132	120	105
$[CdL_2]\cdot(H_2O)_3$	2.22	2.42	2.37	2.62	2.30	83	168	95	101	136	113	111
$[CdL_2]\cdot(H_2O)_4$	2.23	2.35	2.39	2.64	2.31	81	164	98	93	130	107	123
Large Model System												
$[ZnL_2]\cdot(H_2O)_4$	2.05	2.09	2.20	2.59	2.09	85	166	90	96	143	110	124
$[CdL_2]\cdot(H_2O)_4$	2.23	2.31	2.36	2.69	2.30	82	167	94	95	140	93	128

[a] The coordination geometry of the optimized model systems. L_1^{2-} and L_2^{2-} are used for $(CH_3COO)(CH_3S)(im)(H_2O)^{2-}$ and $(CH_3COO)(CH_3S)(im)(H_2O)_2^{2-}$, respectively. O1 is the oxygen atom in Wat1 coordinating to the metal ion; similar notation is used for O2, O103, S181, and N223. The B3LYP/LanL2DZ method was applied in the geometry optimizations. Selected structures are shown in Figures 1−4.

the Cd^{2+}−Asp103 and in particular Cd^{2+}−Cys181 bond lengths decrease by 0.06 and 0.10 Å to 2.24 and 2.50 Å, respectively. The Cd^{2+}−Wat1/His223 bond lengths are almost unaltered. Compared to the corresponding zinc-containing structure, the bond lengths are 0.14−0.22 Å larger. Most of the valence angles are very similar, but the O1−S181 and O1−N223 angles differ by 14° and 20°, respectively.

The following six rows in the table show the optimized structures of the small model systems including the hydrogen-bonding network. They contain either 2, 3, or 4 additional (noncoordinating) water molecules as described in the Methods section. These solvent molecules form hydrogen bonds to the metal ion-coordinating ligands in the crystal structure. All of the optimized $[ZnL_2]\cdot(H_2O)_n$, $n = 2-4$, structures are five-coordinated. They all have an almost trigonal bipyramidal coordination geometry with Asp103 and Wat2 in the apical positions. The additional water molecules for $n = 2$ make hydrogen bonds to Asp103. The additional water molecule for $n = 3$ makes a hydrogen bond to Wat1, and the Zn^{2+}−Wat1 bond length decreases by 0.07 Å compared to $n = 2$. Similarly, the additional water molecule for $n = 4$ makes a hydrogen bond to Wat2, and the Zn^{2+}−Wat2 bond length decreases by 0.11 Å compared to $n = 3$.

For the cadmium-containing systems, the trends are similar to those found for the zinc-containing systems, except for $n = 2$, which has a markedly different structure from the $n = 3$ and $n = 4$ structures and from the zinc-containing structure with $n = 2$. The Cd^{2+}−Wat1 bond length is unusually long (2.44 Å), and the Asp103−Cd^{2+}−Wat2 angle is smaller by about 20° than those in the other model systems. Compared to the small model system, $[CdL_2]$, the Cd^{2+}−Wat1/Cys181/His223 bond lengths for $n = 3$ and $n = 4$ are generally very similar, whereas the Cd^{2+}−Asp103 bond length becomes longer (by up to 0.09 Å for $n = 4$) and the bond length Cd^{2+}−Wat2 becomes shorter (by up to 0.17 Å for $n = 4$).

The two final rows of the table show the optimized structure of the large zinc- or cadmium-containing model systems. For the zinc-containing systems, the Zn^{2+}−Wat2 bond length decreases to 2.09 Å, which is about 0.1 Å shorter than that for the model system without the backbone constraints. The Zn^{2+}−Cys181 bond length increases to 2.59 Å, which is about 0.1 Å longer than that for the model system without the backbone constraints. The valence angles show minor changes, except Wat1−Zn^{2+}−Cys181, which increases by 15° as compared to that in the model system without the backbone constraints. For the cadmium-containing system, the same trends are observed though not as pronounced as for the zinc-containing system. In addition, the Cys181−Cd^{2+}−His223 angle decreases by 14° as compared to that of the model system without the backbone constraints.

TABLE 2: EFGs of Optimized Cd^{2+} Containing Model Systems[a]

	EFG (au)		
	$\lvert V_{xx}\rvert$	$\lvert V_{yy}\rvert$	$\lvert V_{zz}\rvert$
Small Model System			
$[CdL_1]$	0.49	1.01	**1.50**
$[CdL_2]$	0.03	0.81	0.84
Small Model System Including Hydrogen-Bonding Network			
$[CdL_2]\cdot(H_2O)_2$	0.13	0.80	0.93
$[CdL_2]\cdot(H_2O)_3$	0.39	0.44	0.83
$[CdL_2]\cdot(H_2O)_4$	0.24	0.31	0.55
Large Model System			
$[CdL_2]\cdot(H_2O)_4$	0.08	0.49	0.56
PAC Experiment			
5/B/6	0.31	0.63	0.93
569/H/9	0.23	0.57	0.81

[a] The experimental EFGs from the two strains 5/B/6 and 569/H/9 from ref 9 are given at the bottom of the table. L_1^{2-} and L_2^{2-} are used for $(CH_3COO)(CH_3S)(im)(H_2O)^{2-}$ and $(CH_3COO)(CH_3S)(im)(H_2O)_2^{2-}$, respectively. EFGs are calculated at the B3LYP/S & K + 6-31G(d)//B3LYP/LanL2DZ level. The components differing more than 0.5 au from the experimental EFGs are shown in bold face.

3.2. Electric Field Gradients (EFG) at the Metal Ion Binding Sites. In Table 2, the experimentally derived[9] and the calculated EFGs at the position of the cadmium nucleus for the cadmium-containing model systems of site 2 are presented. The last two rows show the results derived from PAC experiments performed on two different strains, 5/B/6 and 569/H/9, of metallo-β-lactamase from *B. cereus*. When comparing experiments and calculations, we wish to be able to reject a given suggested coordination geometry. Therefore, we compare the experiment that is closest to the calculated EFG, and if the difference is large, we can be fairly certain that this coordination geometry is not found in the protein.

The EFG of the four-coordinated small model system, $[CdL_1]$, deviates by up to 0.57 au from experiment. For the five-coordinated structures obtained for the small model system ($[CdL_2]$) and the model systems including the hydrogen-bonding

TABLE 3: Tests of Different Basis Sets for Geometry Optimizations at the B3LYP Level[a]

	distance to the metal ion (Å)					angle subtended at the metal ion (deg)						
	O1	O2	O103	S181	N223	O103−O1	O103−O2	O103−S181	O103−N223	O1−S181	S181−N223	N223−O1
Small Model System												
$[CdL_1]^b$	2.26		2.24	2.50	2.33	85		133	95	127	114	91
$[CdL_1]^c$	2.33		2.22	2.47	2.37	90		123	98	123	117	89
$[CdL_1]^d$	2.32		2.20	2.47	2.35	90		130	99	122	118	89
$[CdL_1]^e$	2.36		2.23	2.47	2.37	89		132	97	122	117	88
$[CdL_2]^b$	2.24	2.52	2.30	2.60	2.30	83	163	122	84	120	114	123
$[CdL_2]^c$	2.33	2.58	2.26	2.54	2.36	87	159	123	85	121	120	111
$[CdL_2]^d$	2.33	2.58	2.25	2.53	2.35	88	159	123	85	121	120	111
$[CdL_2]^e$	2.32	2.90	2.25	2.52	2.35	88	159	128	87	118	117	112
Small Model System Including Hydrogen-Bonding Network												
$[CdL_2]\cdot(H_2O)_3{}^b$	2.22	2.42	2.37	2.62	2.30	83	168	95	101	136	113	111
$[CdL_2]\cdot(H_2O)_3{}^c$	2.30	2.50	2.31	2.57	2.35	86	160	103	101	128	120	107
$[CdL_2]\cdot(H_2O)_3{}^e$	2.31	2.54	2.33	2.55	2.35	87	164	104	99	133	118	105
$[CdL_2]\cdot(H_2O)_3{}^e$	[2.31]	[2.63]	[2.27]	[2.49]	[2.32]	[87]	[162]	[107]	[99]	[135]	[117]	[102]

[a] The coordination geometry of the optimized model systems. L_1^{2-} and L_2^{2-} are used for $(CH_3COO)(CH_3S)(im)(H_2O)^{2-}$ and $(CH_3COO)(CH_3S)(im)(H_2O)_2^{2-}$, respectively. O1 is the oxygen atom in Wat1 coordinating to the metal ion; similar notation is used for O2, O103, S181, and N223. Numbers in brackets represent the structures optimized at the Hartree−Fock level. [b] Optimized using the LanL2DZ basis. [c] Optimized using LanL2DZ on Cd^{2+} and 6-31G(d) on the rest of the atoms. [d] Optimized using LanL2DZ and one additional p and f function on Cd^{2+} (see Method section) and 6-31G(d) on the rest of the atoms. [e] Optimized using LanL2DZ on Cd^{2+} and 6-31+G(d) on the rest of the atoms.

network ($[CdL_2]\cdot(H_2O)_n$, $n = 2-4$), the EFG is reduced and gives much better agreement with experiment. Particularly, the model system with three additional water molecules ($n = 3$) agrees well with experiment (differences of less than 0.13 au). Reasonable agreement is also obtained for the large model system. The eigenvalues of the EFG tensor differ by up to 0.25 au from the experimental values.

3.3. Methods and Basis Sets. To test the quality of the basis sets used in this work, a number of larger basis sets were applied in the geometry optimizations of the four-coordinated complex ($[CdL_1]$), the five-coordinated small model system ($[CdL_2]$), and a model system including selected parts of the hydrogen-bonding network ($[CdL_2]\cdot(H_2O)_3$), see Table 3. For the $[CdL_1]$ complex, the coordination geometries are quite similar applying the different basis sets. The largest difference in geometry is an increase of the Cd−Wat1 bond length from 2.26 to 2.36 Å when applying 6-31G+(d) on the ligands instead of LanL2DZ. The other bond lengths differ by less than 0.04 Å. All of the valence angles generally differ by less than 5°. For the $[CdL_2]$ complex, the following results were found: When applying the 6-31G(d) basis set on the ligands instead of LanL2DZ, the structure remains a distorted trigonal bipyramid (five-coordinated). The changes in Cd^{2+}−ligand bond length are in general about 0.05 Å. However, the Cd^{2+}−Wat1 bond length increases by 0.09 Å from 2.24 to 2.33 Å. Adding a p and an f function to the LanL2DZ basis has almost no effect—changes in Cd^{2+}−ligand bond lengths of less than 0.01 Å. When applying the 6-31+G(d) basis, the structure changes dramatically. Wat2 leaves the first coordination sphere (Cd^{2+}−Wat2 = 2.90 Å), whereas the other ligands bind in a similar coordination geometry as compared to the geometry obtained when using 6-31G(d) on the nonmetal atoms. For the $[CdL_2]\cdot(H_2O)_3$ complex, the coordination geometries remain five-coordinated independent of which basis is used. That is, for the model system including the hydrogen-bonding network, the structure was not as sensitive to the choice of basis set: When applying 6-31G(d) on the nonmetal atoms instead of LanL2DZ, particularly the Cd^{2+}−Wat1 and Cd^{2+}−Wat2 bond lengths change. Both increase by an amount of 0.08 Å—Wat1 from 2.22 to 2.30 Å and Wat2 from 2.42 to 2.50 Å. Using 6-31+G(d) instead of 6-31G(d) on the ligands causes differences of less than 0.04 Å—the Cd^{2+}−Wat2 bond length changes from 2.50 to 2.54 Å. At the Hartree−Fock level, the Cd^{2+}−Wat2 distance increases by 0.09 Å to 2.63 Å, as compared to the B3LYP calculation. This is a very long cadmium−water bond length. The other bond lengths differ by about 0.05 Å from the structure obtained at the B3LYP level.

TABLE 4: EFGs of Cd^{2+} Model Systems Optimized with Different Basis Sets[a]

	EFG (au)		
	$\lvert V_{xx}\rvert$	$\lvert V_{yy}\rvert$	$\lvert V_{zz}\rvert$
Small Model System			
$[CdL_1]^b$	0.49	1.01	1.50
$[CdL_1]^c$	0.51	1.05	1.56
$[CdL_1]^d$	0.50	1.07	1.57
$[CdL_1]^e$	0.48	1.13	1.61
$[CdL_2]^b$	0.03	0.81	0.84
$[CdL_2]^c$	0.47	0.75	1.21
$[CdL_2]^d$	0.49	0.75	1.23
$[CdL_2]^e$	0.54	0.83	1.37
Small Model System Including Hydrogen Bonding Network			
$[CdL_2]\cdot(H_2O)_3{}^b$	0.39	0.44	0.83
$[CdL_2]\cdot(H_2O)_3{}^c$	0.18	0.77	0.95
$[CdL_2]\cdot(H_2O)_3{}^e$	0.30 (0.45) [0.46]	0.76 (0.59) [0.93]	1.06 (1.04) [1.39]

[a] EFGs calculated at the B3LYP/S & K + 6-31G(d) level for the geometry optimized structures obtained with different basis sets (Table 3). L_1^{2-} and L_2^{2-} are used for $(CH_3COO)(CH_3S)(im)(H_2O)^{2-}$ and $(CH_3COO)(CH_3S)(im)(H_2O)_2^{2-}$, respectively. Unless otherwise stated, the second sphere water molecules were not included in the calculation of the EFG. The numbers in parentheses have the second sphere water molecules included in the EFG calculations. In brackets, the EFGs calculated at the Hartree−Fock level are presented. [b] Geometry obtained by optimizing at the B3LYP level with LanL2DZ on all atoms. [c] Geometry obtained by optimizing at the B3LYP level with LanL2DZ on Cd^{2+} and 6-31G(d) on the rest of the atoms. [d] Geometry obtained by optimizing at the B3LYP level with LanL2DZ and one additional p and f function on Cd^{2+} (see Methods section) and 6-31G(d) on the rest of the atoms. [e] Geometry obtained by optimizing at the B3LYP level with LanL2DZ on Cd^{2+} and 6-31+G(d) on the rest of the atoms.

In Table 4, we have listed the EFGs calculated at the position of the cadmium nucleus for the geometries optimized with different basis sets (Table 3). For the four-coordinated $[CdL_1]$ complexes, the EFGs are generally very similar. The largest difference is observed for the V_{yy} and V_{zz} components, which increase by 0.12 au and 0.11 au, respectively, for the structure obtained by optimizing with the 6-31G+(d) on the ligands instead of the LanL2DZ basis set. Not surprisingly, large variations in EFGs are observed for the five-coordinated $[CdL_2]$

complex because the geometries differ substantially, see Table 3. Differences of the EFG components of about 0.4 au are observed between the structures optimized with LanL2DZ and 6-31G(d) on the ligands. For example, the V_{zz} component changes from 0.84 au to 1.21 au. For the structure optimized with the 6-31+G(d) basis, even larger differences from the structure optimized with the LanL2DZ basis are observed. For the $[CdL_2]\cdot(H_2O)_3$ complexes, the largest difference of 0.33 au is observed for the V_{yy} component between the structures optimized with LanL2DZ and 6-31G(d) on the ligands. The V_{xx} and V_{zz} components differ by 0.1−0.2 au. Optimizing the structures with 6-31G+(d) instead of 6-31G(d) on the ligands causes differences in the EFG components of less than 0.12 au. When the three second-sphere solvent molecules are included in the EFG calculations, a decrease of the EFG components is observed (0.02−0.2 a.u). Using Hartree−Fock instead of B3LYP for calculating the EFGs (for the structure optimized at the B3LYP level) increases the EFG by up to 0.33 au (the V_{zz} component).

Calculations using the contracted instead of the uncontracted basis set of Sadlej and Kellö were also performed. However, the fourth s-type orbital in the basis was discarded when the default settings of Gaussian 98 for checking for linear dependencies was used. A test calculation with the contracted basis set in which the routine checking for linear dependencies was disabled gave rise to only small differences of less than 0.03 au in EFGs. The differences between the EFGs calculated with the contracted and uncontracted basis sets were smaller than 0.04 au. Test calculations using 10^{-8} au instead of 10^{-5} au as the convergence criterion for the rms of the elements of the density matrix caused differences of less than 0.03 au. This was also tested in ref 30 for linear Cd complexes in which even smaller differences of less than 0.005 au in the EFG for different convergence criteria are observed.

4. Discussion

In this work, β-lactamase with one metal ion (Zn^{2+} or Cd^{2+}) bound at the site with His223, Asp103, Cys181, and 1−2 water molecules as ligands (site 2) has been studied with first principle quantum mechanical methods in terms of metal ion coordination geometry and EFGs. We chose to construct the mononuclear site 2 from the binuclear 1ZNB structure from *B. fragilis* and to use it as starting point for the geometry optimizations because no structure is available in which only site 2 is occupied. A number of model systems are used: (1) the metal ion and the coordinating ligands (the small model systems), (2) the metal ion, the coordinating ligands, and the local hydrogen-bonding network (the small model systems including the hydrogen-bonding network), and (3) the metal ion, the coordinating ligands, the local hydrogen-bonding network, and the constraints from the surrounding protein (the large model systems). These different types of model systems were studied to evaluate the importance of the hydrogen-bonding network and the backbone constraints. The results will be compared to experimental data recorded on the enzyme of *B. cereus*, which is very similar to *B. fragilis*. The metal ion-coordinating residues are the same, and the amino acids included in the large model system are the same except Gly102, which is an alanine in *B. cereus*. Thus, the model systems can be assumed to be almost equally good for the metal ion binding sites of the two proteins. Differences between the two enzymes further away from the metal ion binding sites are not taken into account in this work.

Recent experimental studies show that either of the two binding sites in metallo-β-lactamase can be occupied at low metal ion to enzyme concentration,[9] and it is not clear what role site 2 plays in the catalytic mechanism for the enzyme with only one metal ion bound.[17] Previously, it has been assumed that the site with three histidines was responsible for catalysis. However, as described in the Introduction, a number of recent publications indicate that this conventional picture of site 1 as the catalytically active site is too simple.[9,17,19] These recent experimental data indicate, surprisingly, that site 2 may participate as an integral part of the mechanism for the mononuclear enzyme. In addition, metallo-β-lactamase from *B. cereus* binds one metal ion strongly and the second more weakly, so the enzyme with only one metal ion bound may be the physiologically relevant species. Therefore, it is important to elucidate the coordination geometry of site 2 as a prerequisite for understanding how it can be involved in the catalytic mechanism of the enzyme. In particular, because X-ray crystallographic data are inconclusive,[1−9] the following questions remain: Is the site four- or five-coordinated? Is it a real physical effect that Wat2 can move on and off as a ligand at little energetic cost? Does this have implications for the understanding of the catalytic mechanism? We shall address these questions in the following.

4.1. Structure of the Metal Ion Binding Site. In many publications on metal ion binding sites of metalloproteins, a model system of similar or smaller size than our "small" systems is used (see, for example, refs 21,22,25). Our results indicate that this is too small a system to model site 2 of metallo-β-lactamase properly, see Tables 1 and 3. For the native Zn^{2+}-containing enzyme, the small model system becomes four-coordinate when optimized, even though the starting point is the five-coordinated structure determined by X-ray crystallography (1ZNB). The second water molecule, Wat2, leaves the first coordination sphere and makes a hydrogen bond to the aspartate or the cysteinate residue. Similar results were obtained by Diaz et al.[21] So a possible conclusion is that the site is four-coordinated in the mononuclear enzyme (the X-ray data were recorded for the binuclear enzyme). However, upon introduction of the surrounding hydrogen-bonding network into the optimization, the optimized structure remains five-coordinated. It was checked that this structure represents an energy minimum on the potential energy surface by a frequency calculation. A five-coordinated structure is also obtained for the optimizations in which both the backbone constraints and the hydrogen-bonding network are included. The fact that the best models of the metal ion binding sites give a five-coordinated structure indicates that this is also the structure present in the protein. Most crystal structures support the existence of a five-coordinated site 2,[1,3,7,8,4] though they are not directly comparable to our calculations because they represent binuclear enzymes. However, there are two crystal structures with a four-coordinated site 2.[9,31] In ref 9, however, the structure is remarkably similar to the five-coordinated one, that is, a trigonal bipyramid but with one of the apical ligands (Wat2) missing. We suggest that inclusion of Wat2 in the fitting of the X-ray diffraction data would be appropriate also for this structure.

Further information on the coordination geometry is provided by PAC spectroscopy[9] from which the EFG at the site of the cadmium nucleus can be derived. The geometry was optimized and EFGs were calculated for the cadmium ion-containing model systems and compared with experimentally determined EFGs for these systems, see Table 4. The only calculated EFG that deviates more than 0.5 au from experiment is the one found for the four-coordinated structure. Therefore, it is very unlikely that this is the real structure in the cadmium ion-containing β-lactamase with only one metal ion bound. Consequently, these are strong indications that site 2 is five-coordinated and that

the inclusion of the surrounding hydrogen-bonding network is essential for the proper modeling of the site 2 in β-lactamase.

4.2. Flexibility of the Metal Ion Binding Site. The fact that the inclusion of the hydrogen-bonding network has such a large impact on the coordination geometry in itself indicates that this is a flexible metal ion binding site, at least for some of the ligands. The two water molecules are, not surprisingly, particularly affected. The structures of the $[CdL_2]$ complex optimized with 6-31G(d) and 6-31+G(d) on the ligands primarily differ by an increase of the Cd^{2+}−Wat2 bond length of 0.38 Å. The energy difference (calculated with the same basis set as in the EFG calculations, see Method section) between these two structures is only about 1 kcal/mol. Diaz et al.[21] also conclude that the position of Wat2 is flexible. The flexible position of Wat2 might indicate that this serves as a storage position for water molecules to be consumed in the chemical process. Alternatively, Concha et al.[1,3] propose that Wat2 acts as a proton donor to the β-lactam amide. The flexible position of Wat2 is in good agreement with this proposal because it indicates that not much energy is needed to position Wat2 optimally.

The position of Wat1 also varies, depending on the inclusion of the water molecule (Wat5) that hydrogen bonds to it. This water molecule is probably not present when the substrate is bound, and a flexible position of Wat1 might be advantageous for orienting it optimally to make a nucleophilic attack on the carbonyl carbon in the lactam ring.

Introducing the backbone constraints reveals another interesting feature: The Zn^{2+}−Cys181 bond length increases by 0.11 Å. In addition, the sulfur of the cysteinate is moved in the plane of the trigonal bipyramid, away from Wat1 and toward His223 by 10−16°, see Table 1. This protein-controlled positioning of the cysteine residue might also be related to the mechanism of the enzyme.

4.3. Differences between Zinc- and Cadmium-Containing Model Systems. In contrast to the small model system containing zinc, it is possible to obtain a five-coordinated structure with cadmium as the metal ion, even without the hydrogen-bonding network. Probably, the larger radius of the cadmium ion makes it possible. However, as seen from the relatively large Asp103−Cd^{2+}−Cys181 angle of 122° (see Table 1), the position of the cysteine residue is distorted from the trigonal bipyramidal geometry observed in the crystal structure. The reason may be electrostatic repulsion between these two formally negatively charged residues. In addition, there is a hydrogen bond between Cys181 and Wat2. The cadmium-containing model systems with three or four additional water molecules ($[CdL_2]\cdot(H_2O)_n$, n = 3,4) are similar to the zinc-containing systems. Only the bond lengths differ because of the larger size of the cadmium ion causing 0.14−0.22 Å longer Cd−ligand bond lengths. The valence angles differ by less than 5°. However, the complex with only two additional water molecules (n = 2) shows significant differences between the zinc- and cadmium-containing structures. In particular, the metal ion−Wat1 bond length differs by as much as 0.34 Å, and the Asp103−M−Wat2 angle differs by 19°. This may be due to the fact that there is a hydrogen bond between Wat1 and Wat2 in the $[CdL_2]\cdot(H_2O)_2$ complex, which is not present with n = 3,4. This emphasizes the sensitivity of this site to the surroundings and indicates that it is necessary to include more than two additional water molecules to get an appropriate model for the cadmium-containing system.

4.4. Quality and Accuracy of the Calculations. It is necessary to estimate the accuracy of the applied methods, in particular, because we have used the relatively small LanL2DZ basis set for geometry optimizations.

In Table 3, it is observed that the metal ion−ligand bond lengths change by less than 0.09 Å and the valence angles change by less than 12° when applying the 6-31G(d) and 6-31+G(d) basis sets instead of LanL2DZ, except in one case, $[CdL_2]$ with 6-31+G(d) on the ligands, in which the Cd−Wat2 bond length increases by as much as 0.38 Å to 2.90 Å. A bond length of 2.52 Å for Cd−H_2O is in itself very long, and 2.90 Å means that the water molecule has effectively left the first coordination sphere. However, by including the hydrogen-bonding network, this water molecule stays in the first coordination sphere. This means that caution should be exercised when comparing structures and EFGs of the small five-coordinated model systems with experiment. It is important to note that both the structure and EFG for the four-coordinated site is fairly insensitive to the choice of the basis set. In particular, the EFG is in all cases relatively large and significantly different from the experimental value. On the basis of the other results in Table 3, we estimate that the inaccuracy is about 0.1 Å for Cd^{2+}−ligand bond lengths and 10° for the valence angles using B3LYP/LanL2DZ. Similarly, on the basis of the results in Table 4, we estimate that the inaccuracy of the EFG calculation is 0.3−0.4 au. The latter is in good agreement with previously published evaluations of calculated EFGs.[25−28]

For future studies, when larger computer resources are available, it can be noted that using an all-electron basis set with polarization functions on the ligands will be better with respect to determination of the structure. But, surprisingly, addition of diffuse functions has a small effect even for the charged ligands, cysteinate and aspartate. Addition of polarization functions, one p- and one f-type basis function, on cadmium only has a minor effect on the structure.

Applying the Hartree−Fock method instead of the B3LYP has an effect of 0.05−0.10 Å on the Cd^{2+}−ligand bond lengths and 5°−10° on the valence angles. Similar results were found by Diaz et al.[21] on a smaller model system: $[Zn(HCOO)(NH_3)(SH)(H_2O)_2]$. In addition, Diaz et al. optimized the structure with the MP2 method, which gave results close to those of the B3LYP method. Therefore, it seems to be optimal to apply the latter.

5. Conclusion

The structure and EFGs of different model systems of site 2 of metallo-β-lactamase, with only one metal ion bound, have been studied with either zinc or cadmium as the metal ion. Model systems with only the metal ion coordinating ligands (small model systems) have been considered, and furthermore, the environment has been modeled by including second sphere solvent molecules (model systems including the hydrogen-bonding network) and by extending the molecular system to include the backbone constraints (large model systems).

It was not possible to optimize a five-coordinated complex for the zinc ion-containing small model system. Wat2 left the first coordination sphere, and the result was a four-coordinated structure. However, inclusion of the hydrogen-bonding network gave a structure in good agreement with X-ray diffraction data (see below). Therefore, we conclude that it is important to include the hydrogen-bonding network for the appropriate modeling of the coordination geometry.

The experimental EFGs can be reproduced: The five-coordinated model systems generally deviate by less than 0.3 au from the experimental PAC data, and in particular, for the complex with three additional second sphere solvent molecules,

$[CdL_2]\cdot(H_2O)_3$, good agreement is obtained. This indicates that these model systems have coordination geometries that are similar to the one found in the enzyme. For the four-coordinated structure, however, disagreement by up to 0.6 au for the EFG tensor components is observed, leading to the conclusion that this model system does not represent the cadmium-substituted site 2 well. Accordingly, there seems to be strong evidence for a five-coordinated cadmium ion-containing site 2.

The structural differences of the metal ion binding site for the different model systems reveal a very flat potential energy surface with very variable positions of, particularly, Wat1, Wat2, and Cys181. This may be related to the mechanism of the enzyme.

Acknowledgment. This work was supported by a TMR network of the European Union (CT-0232), the Danish Natural Science Research Council, the Danish Technical Research Council, and the Carlsberg Foundation. We thank Professor Rogert Bauer for useful discussions.

References and Notes

(1) Concha, N. O.; Rasmussen, B. A.; Bush, K.; Herzberg, O. *Structure* **1996**, *4*, 823.
(2) Carfi, A.; Duée, E.; Paul-Soto, R.; Galleni, M.; Frère, J.-M.; Dideberg, O. *Acta Crystallogr.* **1998**, *D54*, 47.
(3) Concha, N. O.; Rasmussen, B. A.; Bush, K.; Herzberg, O. *Protein Sci.* **1997**, *6*, 2671.
(4) Fitzgerald, P. M. D.; Wu, J. K.; Toney, J. H. *Biochemistry* **1998**, *37*, 6791.
(5) Toney, J. H.; Fitzgerald, P. M. D.; Grover sharma, N.; Olson, S. H.; May, W. J. *Chem. Biol.* **1998**, *5*, 185.
(6) Carfi, A.; Pares, S.; Duée, E.; Galleni, M.; Duez, C.; Frère, J.-M.; Dideberg, O. *EMBO J.* **1995**, *14*, 4914.
(7) Carfi, A.; Duée, E.; Galleni, M.; Frère, J.-M.; Dideberg, O. *Acta Crystallogr.* **1998**, *D54*, 313.
(8) Fabiane, S. M.; Sohi, M. K.; Wan, T.; Payne, D. J.; Bateson, J. H.; Mitchell, T.; Sutton, B. J. *Biochemistry* **1998**, *37*, 12404.
(9) Paul-Soto, R.; Zeppezauer, M.; Adolph, H.-W.; Galleni, M.; Frère, J.-M.; Carfi, A.; Didenberg, O.; Wouters, J.; Hemmingsen, L.; Bauer, R. *Biochemistry* **1999**, *38*, 16500.
(10) Galleni, M.; Lamotte-Brasseur, J.; Rossolini, G. M.; Spencer, J.; Dideberg, O.; Frère, J.-M. *Antimicrob. Agents Chemother.* **2001**, *45*, 660.
(11) Wang, Z.; Fast, W.; Valentine, A. M.; Benkovic, S. J. *Curr. Opin. Chem. Biol.* **1999**, *3*, 614.
(12) Orellano, E. G.; Girardini, J. E.; Cricco, J. A.; Ceccarelli, E. A.; Vila, A. J. *Biochemistry* **1998**, *37*, 10173.
(13) Crowder, M. W.; Wang, Z.; Franklin, S. L.; Zovinka, E. P.; Benkovic, S. J. *Biochemistry* **1996**, *35*, 12126.
(14) Wang, Z.; Benkovic, S. J. *J. Biol. Chem.* **1998**, *273*, 22402.
(15) Paul-Soto, R.; Hernandez-Valladares, M.; Galleni, M.; Bauer, R.; Zeppezauer, M.; Frère, J.-M.; Adolph, H. W. *FEBS Lett.* **1998**, *438*, 137.
(16) Damblon, C.; Prosperi, C.; Lian, L.-Y.; Barsukov, I.; Paul-Soto, R.; Galleni, M.; Frère, J.-M.; Roberts, G. C. K. *J. Am. Chem. Soc.* **1999**, *121*, 11576.
(17) Paul-Soto, R.; Bauer, R.; Frère, J.-M.; Galleni, M.; Meyer-Klaucke, W.; Nolting, H.; Rossolini, G. M.; de Seny, D.; Hernandez-Valladares, M.; Zeppezauer, M.; Adolph, H.-W. *J. Biol. Chem.* **1999**, *274*, 13242.
(18) Bounaga, S.; Laws, A. P.; Galleni, M.; Page, M. I. *Biochem. J.* **1998**, *331*, 703.
(19) Hemmingsen, L.; Damblon, C.; Antony, J.; Jensen, M.; Adolph, H. W.; Wommer, S.; Roberts, G. C. K.; Bauer, R. *J. Am. Chem. Soc.* **2001**, *123*, 10329.
(20) Siegbahn, P. E. M.; Blomberg, M. R. A. *Chem. Rev.* **2000**, *100*, 421.
(21) Diaz, N.; Suárez, D.; Merz, K. M., Jr. *J. Am. Chem. Soc.* **2000**, *122*, 4197.
(22) Gilson, H. S. R.; Krauss, M. *J. Am. Chem. Soc.* **1999**, *121*, 6984.
(23) Suárez, D.; Merz, K. M., Jr. *J. Am. Chem. Soc.* **2001**, *123*, 3759.
(24) Krauss, M.; Gilson, H. S. R.; Gresh, N. *J. Phys. Chem. B* **2001**, *105*, 8040.
(25) Ryde, U.; Hemmingsen, L. *J. Biol. Inorg. Chem.* **1997**, *2*, 567.
(26) Hemmingsen, L.; Ryde, U. *J. Phys. Chem.* **1996**, *100*, 4803.
(27) Hansen, B.; Bukrinsky, J. T.; Hemmingsen, L.; Bjerrum, M.; Singh, K.; Bauer, R. *Phys. Rev. B* **1999**, *59*, 14182.
(28) Hemmingsen, L.; Ryde, U.; Bauer, R. *Z. Naturforsch.* **1999**, *54a*, 422.
(29) Hemmingsen, L.; Bauer, R.; Bjerrum, M. J.; Schwarz, K.; Blaha, P.; Andersen, P. *Inorg. Chem.* **1999**, *38*, 2860.
(30) Antony, J.; Hansen, B.; Hemmingsen, L.; Bauer, R. *J. Phys. Chem. A* **2000**, *104*, 6047.
(31) Concha, N. O.; Cheever, C. A.; Clarke, B. P.; Lewis, C.; Galleni, M.; Frére, J.-M.; Payne, P. J.; Bateson, J. H.; Abdel-Megvid, S. S. *Biochemistry* **2000**, *39*, 4288.
(32) Frisch, M. J.; Trucks, G. W.; Schlegel, H. B.; Scuseria, G. E.; Robb, M. A.; Cheeseman, J. R.; Zakrzewski, V. G.; Montgomery, J. A., Jr.; Stratmann, R. E.; Burant, J. C.; Dapprich, S.; Millam, J. M.; Daniels, A. D.; Kudin, K. N.; Strain, M. C.; Farkas, O.; Tomasi, J.; Barone, V.; Cossi, M.; Cammi, R.; Mennucci, B.; Pomelli, C.; Adamo, C.; Clifford, S.; Ochterski, J.; Petersson, G. A.; Ayala, P. Y.; Cui, Q.; Morokuma, K.; Malick, D. K.; Rabuck, A. D.; Raghavachari, K.; Foresman, J. B.; Cioslowski, J.; Ortiz, J. V.; Stefanov, B. B.; Liu, G.; Liashenko, A.; Piskorz, P.; Komaromi, I.; Gomperts, R.; Martin, R. L.; Fox, D. J.; Keith, T.; Al-Laham, M. A.; Peng, C. Y.; Nanayakkara, A.; Gonzalez, C.; Challacombe, M.; Gill, P. M. W.; Johnson, B. G.; Chen, W.; Wong, M. W.; Andres, J. L.; Head-Gordon, M.; Replogle, E. S.; Pople, J. A. *Gaussian 98*, revision A.5; Gaussian, Inc.: Pittsburgh, PA, 1998.
(33) Sprouse, G. D.; Häusser, O.; Andrews, H. R.; Faestermann, T.; Beene, J. R.; Alexander, T. K. *Hyperfine Interact.* **1978**, *4*, 229.
(34) Becke, A. D. *J. Chem. Phys.* **1993**, *98*, 5648.
(35) Dunning, T. H.; Hay, P. J. In *Modern Theoretical Chemistry*; Schaefer, H. F., III, Ed.; Plenum Press: New York, 1976; Vol. 2.
(36) Hay, P. J.; Wadt, W. R. *J. Chem. Phys.* **1985**, *82*, 270.
(37) Wadt, W. R.; Hay, P. J. *J. Chem. Phys.* **1985**, *82*, 284.
(38) Hay, P. J.; Wadt, W. R. *J. Chem. Phys.* **1985**, *82*, 299.
(39) Hehre, W. J.; Ditchfield, R.; Pople, J. A. *J. Chem. Phys.* **1972**, *56*, 2257.
(40) Ditchfield, R.; Hehre, W. J.; Pople, J. A. *J. Chem. Phys.* **1971**, *54*, 724.
(41) Hariharan, P. C.; Pople, J. A. *Mol. Phys.* **1974**, *27*, 209.
(42) Gordon, M. S. *Chem. Phys. Lett.* **1980**, *76*, 163.
(43) Hariharan, P. C.; Pople, J. A. *Theor. Chim. Acta* **1973**, *28*, 213.
(44) Maseras, F.; Morokuma, K. *J. Comput. Chem.* **1995**, *16*, 1170.
(45) Matsubara, T.; Maseras, F.; Koga, N.; Morokuma, K. *J. Phys. Chem.* **1996**, *100*, 2573.
(46) Svensson, M.; Humbel, S.; Froese, R. D. J.; Matsubara, T.; Sieber, S.; Morukuma, K. *J. Phys. Chem.* **1996**, *100*, 19357.
(47) Humbel, S.; Sieber, S.; Morokuma, K. *J. Chem. Phys.* **1996**, *105*, 1959.
(48) Dapprich, S.; Komàromi, I.; Byun, K. S.; Morokuma, K.; Frisch, M. J. *J. Mol. Struct. (THEOCHEM)* **1999**, *461*−*462*.
(49) Stewart, J. J. *J. Comput. Chem.* **1989**, *10*, 209.
(50) Stewart, J. J. *J. Comput. Chem.* **1989**, *10*, 221.
(51) Kellö, V.; Sadlej, A. *Theor. Chim. Acta* **1995**, *91*, 353.